Mitigation of the Brighter-Fatter Effect in LSSTCam

Alex Broughton

ISPA
3/13/2024

Inhomogeneous distributions of charges in potential wells of pixels result in transverse Coulomb forces that displace charges

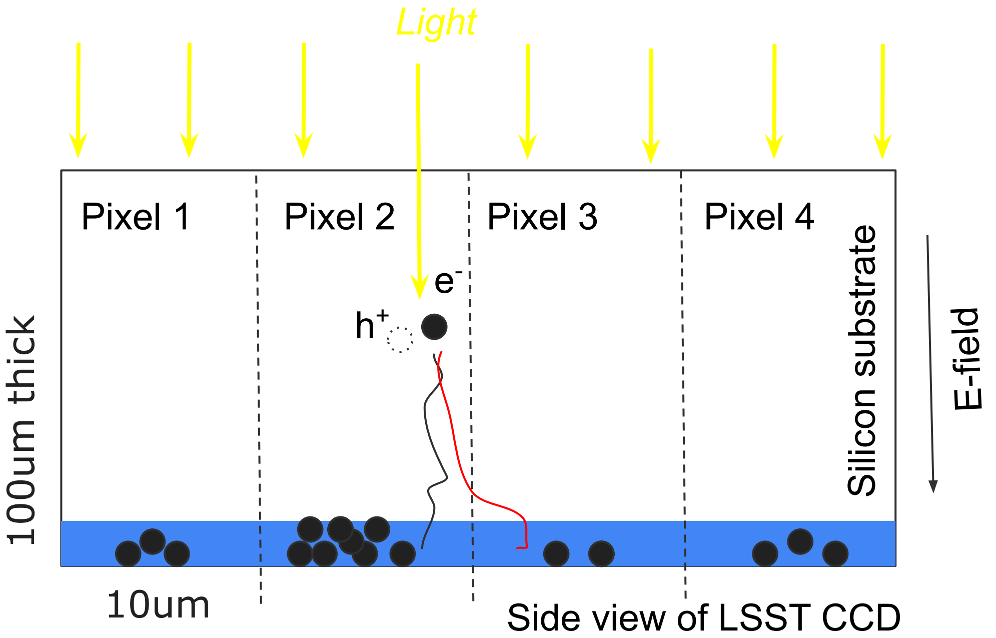

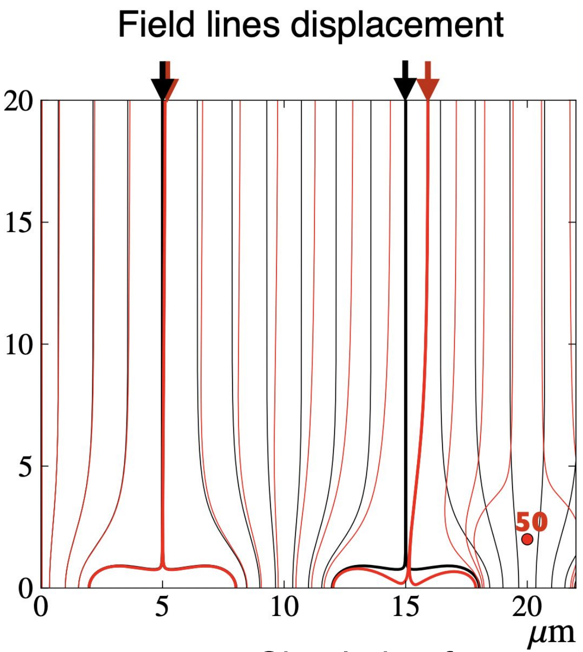

Has been observed in all astrophysical imagers (at least going back to the Wide FIeld Camera/Planetary Camera of HST)

Simulation from Gruen et al. (2015)

The Brighter-Fatter Effect (BFE)

The BFE makes bright sources appear larger.
e.g. PSF estimation, brightest cluster galaxies (BCGs), type Ia SNe, etc.

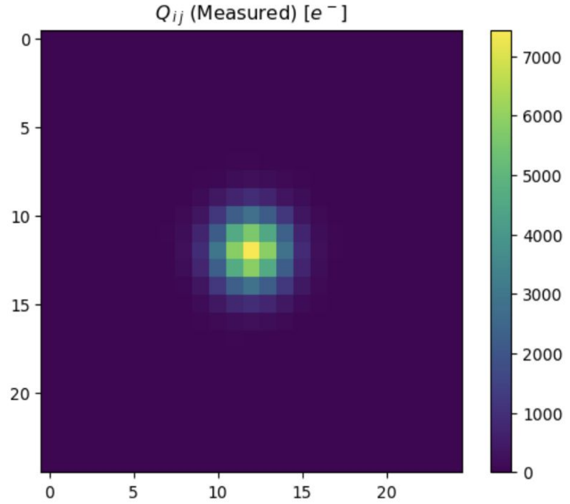

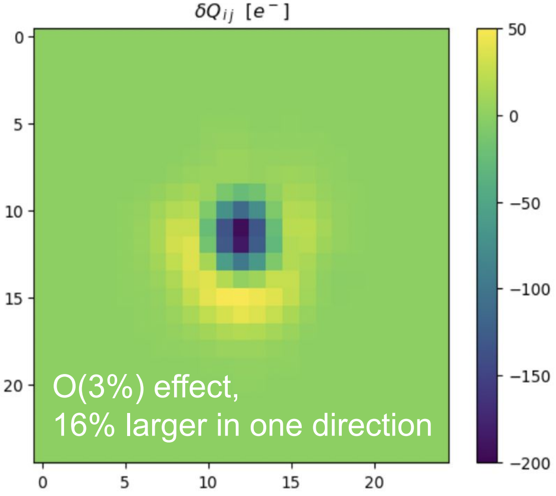

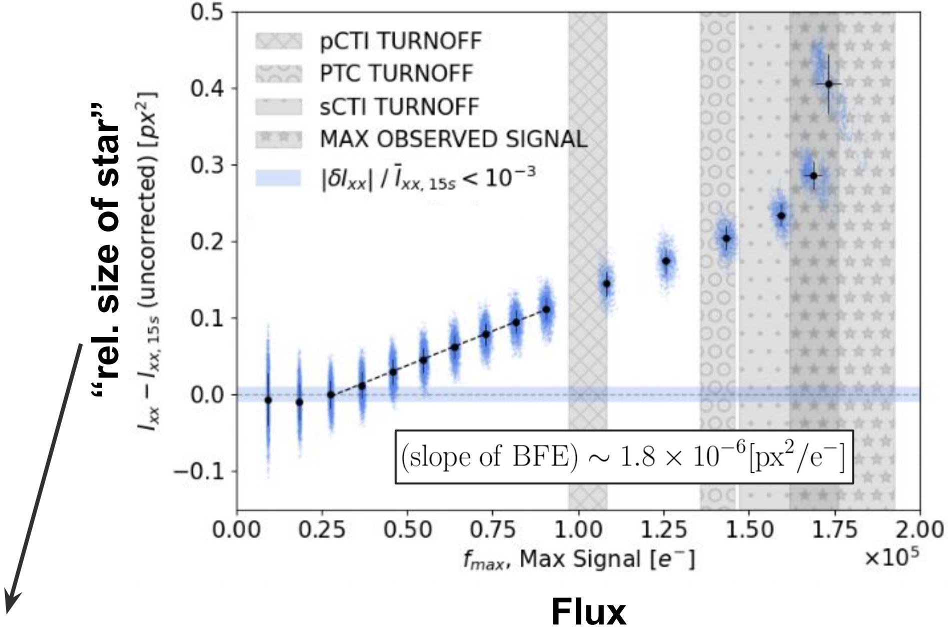

Flux

$$I_{\mu\nu} = 2 \times \frac{\int_{\mathbf{R}^2} (\boldsymbol{x} - \boldsymbol{x}_0)_\mu (\boldsymbol{x} - \boldsymbol{x}_0)_\nu w(\boldsymbol{x}) I(\boldsymbol{x})\, \mathrm{d}^2\boldsymbol{x}}{\int_{\mathbf{R}^2} w(\boldsymbol{x}) I(\boldsymbol{x})\, \mathrm{d}^2\boldsymbol{x}}$$

Pixel-Pixel Correlations in Flat Fields in the LSST Camera

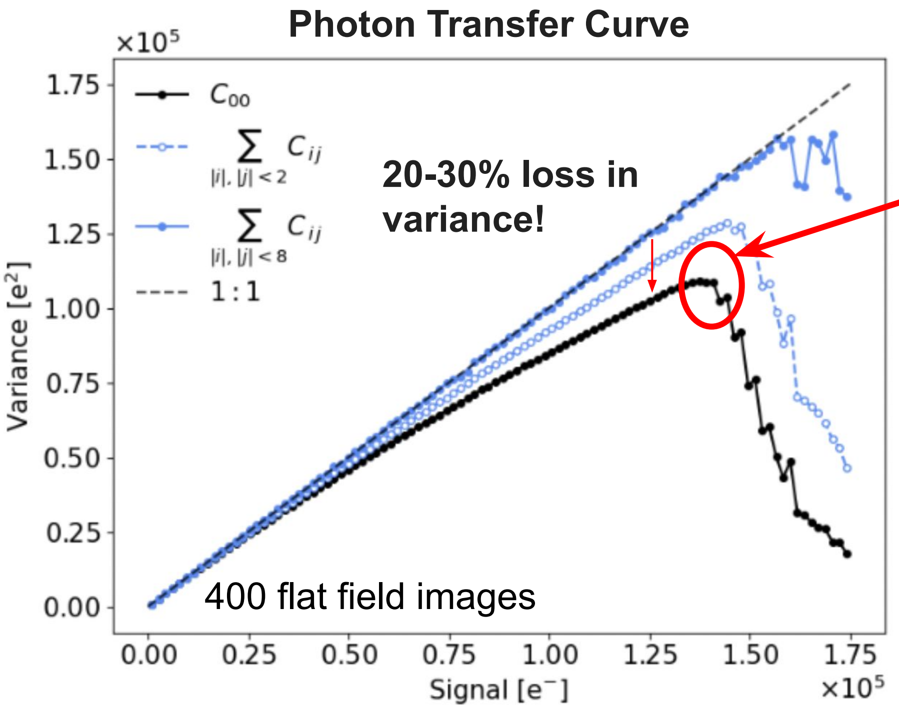

PTC turnoff :
Pixel saturation,
charges move about
freely

Altered charge current can be modeled by changes to the effective pixel area $\dot{Q}_{00} = I[1 + \sum_{kl} a_{kl} Q_{kl}]$

Original Poisson term | *Modified by change in area* | *Higher-order effects* | *Flux-indep. electronic noise*

$$C_{ij}(\mu) = \frac{\mu}{g}\Big[\delta_{i0}\delta_{j0} + a_{ij}\mu g + \frac{2}{3}[\boldsymbol{a} \otimes \boldsymbol{a}]_{ij}(\mu g)^2 + \frac{1}{3}[\boldsymbol{a} \otimes \boldsymbol{a} \otimes \boldsymbol{a}]_{ij}(\mu g)^3 + \cdots\Big] + n_{ij}/g^2$$

Astier et al. (2019)

*g = e^-/ADU

Pixels are distorted in LSST sensors due to charge accumulation

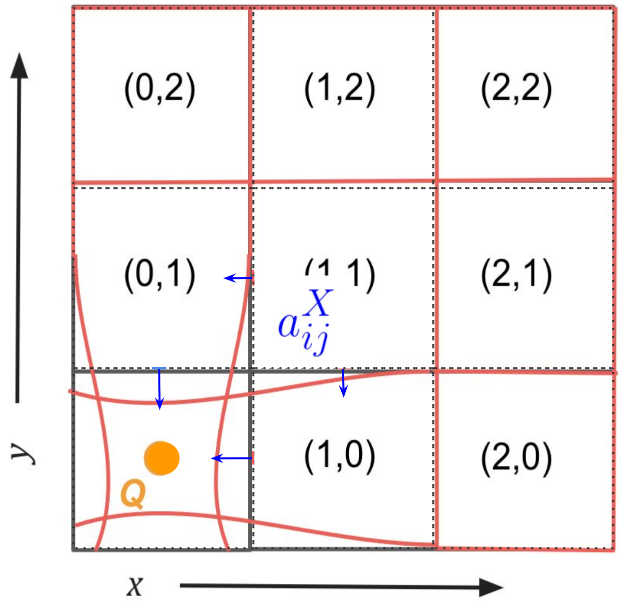

More than 50% of charge displacement happens beyond 4 pixels away!

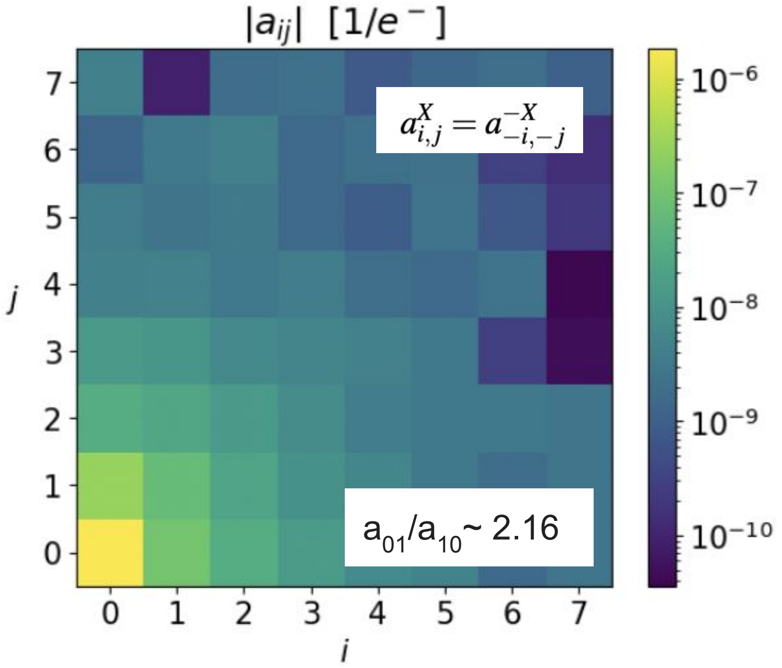

Broughton et al. (2023)

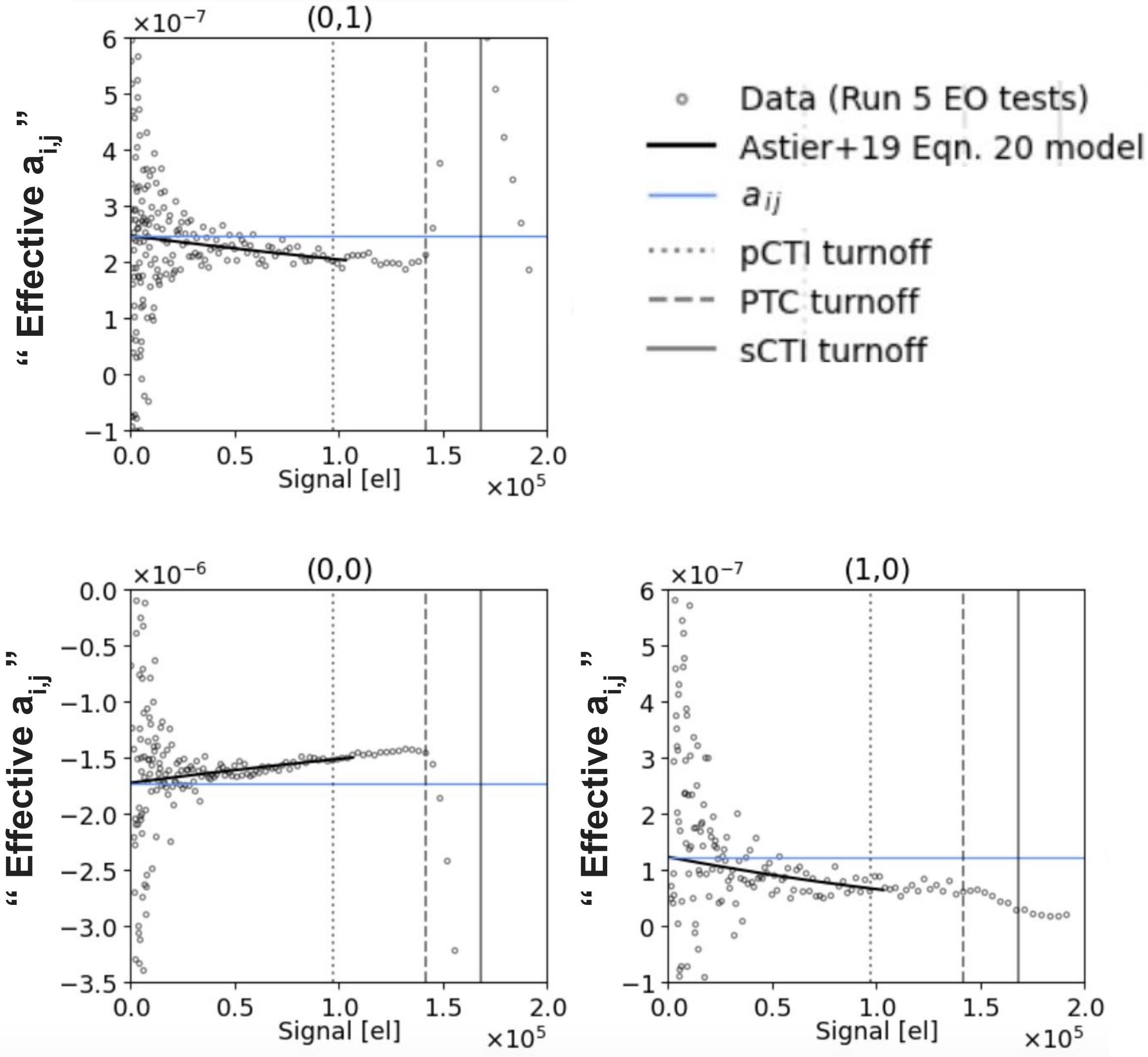

(0,1)
(0,0)
(1,0)
“ Effective a_i,j ”
Signal [el]
Data (Run 5 EO tests)
Astier+19 Eqn. 20 model
a_ij
pCTI turnoff
PTC turnoff
sCTI turnoff

These higher-order effects make up 30% of the total effect near sensor saturation

At low signal levels, the pixel-to-pixel effects are approximated well by a constant fractional area change “matrix”

At high signal levels, the pixel-to-pixel effects are non-trivial and need to be measured empirically.

How well can we correct it?

There are 4 proposed corrections:
Antilogus+14, Gruen+15, Coulton+18, Astier+23

Coulton et al. (2018) is currently implemented in the Rubin Observatory science pipelines for LSSTCam, and used/tested by Hyper-Suprime Cam and Euclid imagers

Currently implemented correction in LSST Science Pipelines

Calculate Covariances → Derive a 2D kernel from covariances → Apply to Image

Pixel-pixel covariances derived from flat field images as a function of flux

$$C(\mathbf{x} - \mathbf{x}') = -\mu^2 \frac{\partial}{\partial x} \cdot \frac{\partial}{\partial x} K$$

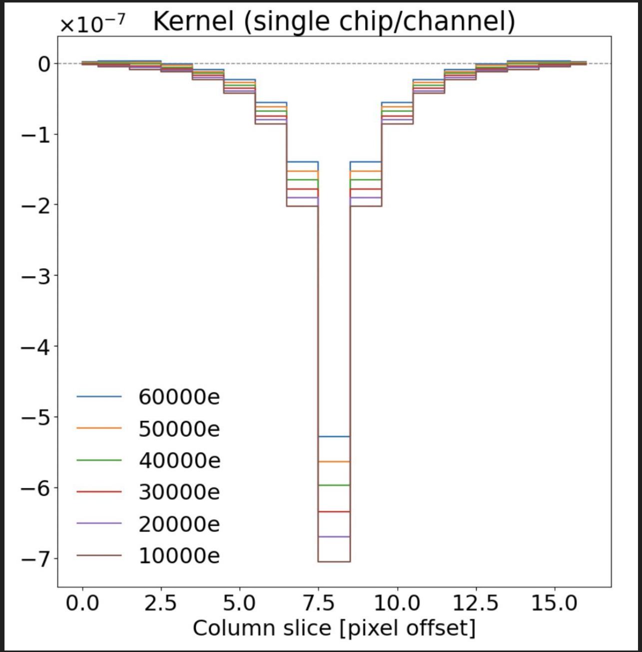

Step 1 $\Phi = F * K$

Step 2 $V = F \nabla \Phi$

Step 3 $\delta F = \frac{1}{2} \nabla \cdot V$

$$\hat{F} = F + \delta F$$

Based on
Coulton et al. 2018
Broughton et al. (2023)

10^4 electrons

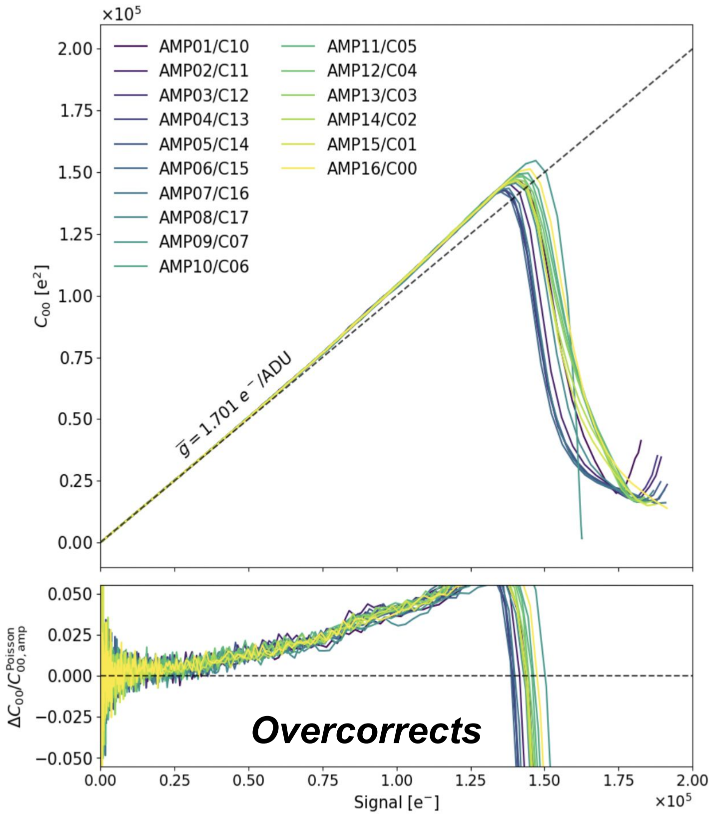

6 x 10^4 electrons

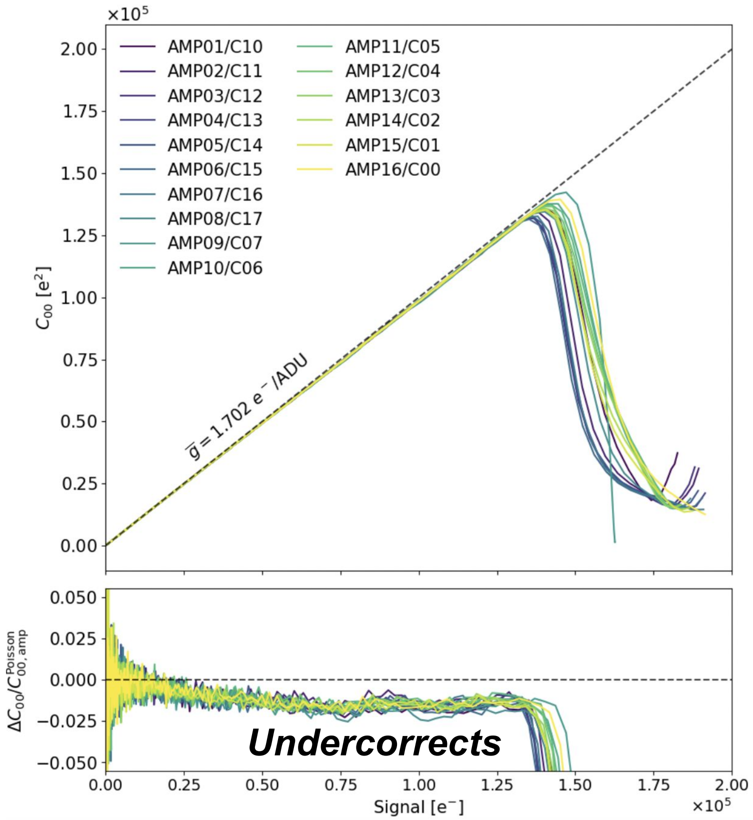

Pick the "ideal" signal level that best reconstructs the Poisson form of the PTC.

Determined by testing a range of signal levels and attempting to minimize the chi^2

$$\chi^2 = \sum_{\mu} (C_{00} - C_{00}^{Poisson})^2 w_{\mu}$$

An unbiased kernel can be determined from flat field statistics

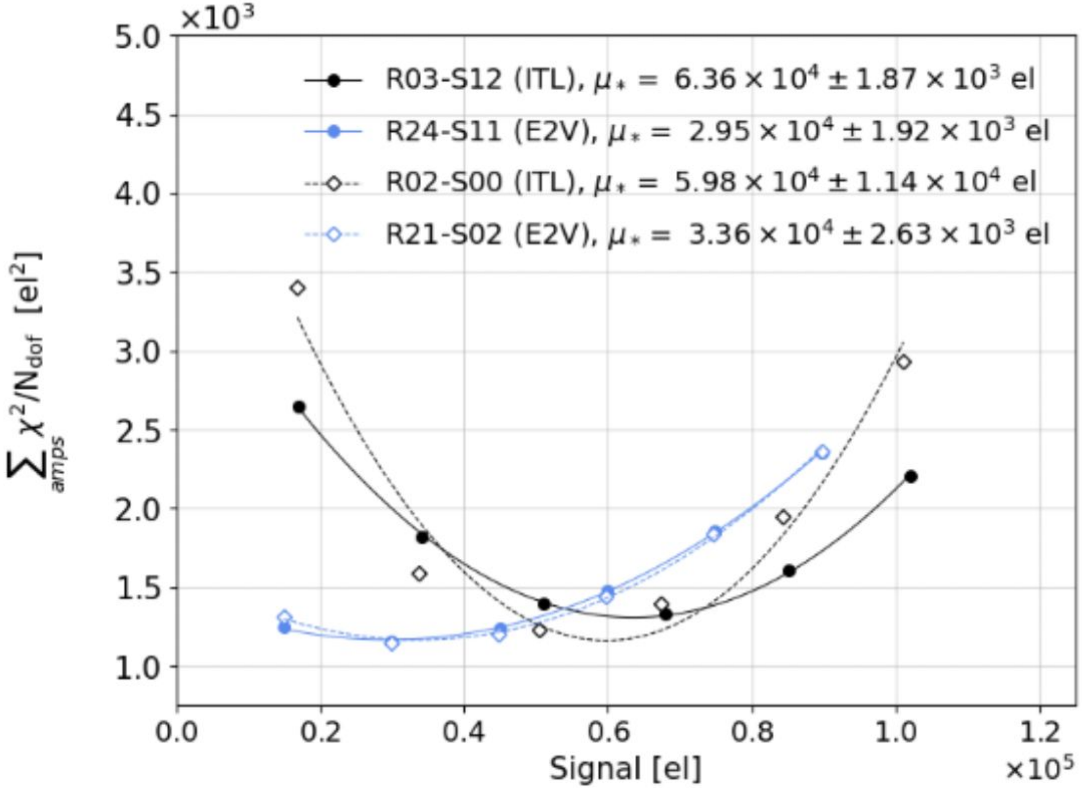

Corrects 94%
of the effect
in flat images

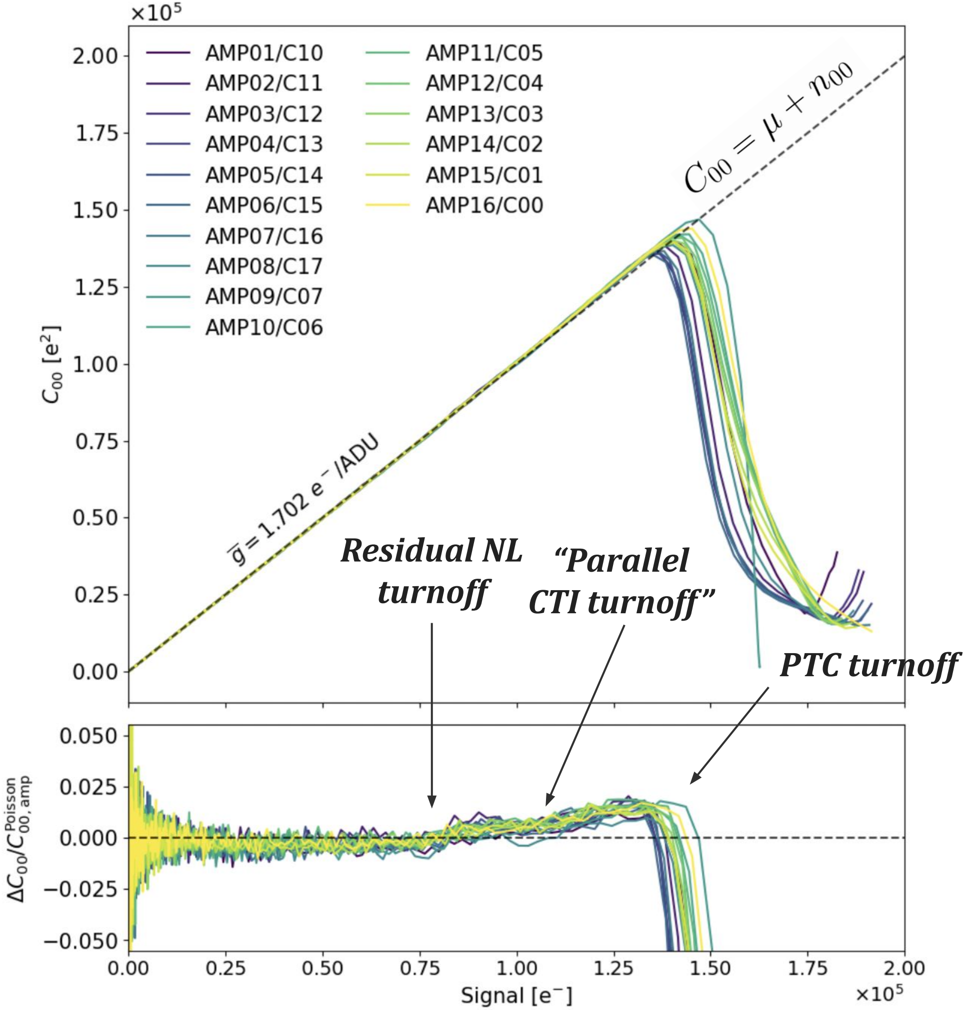

Corrects 90%
of the anisotropy
between x/y

Broughton et al. (2023)

Testing the correction on artificial PSFs using LSSTCam

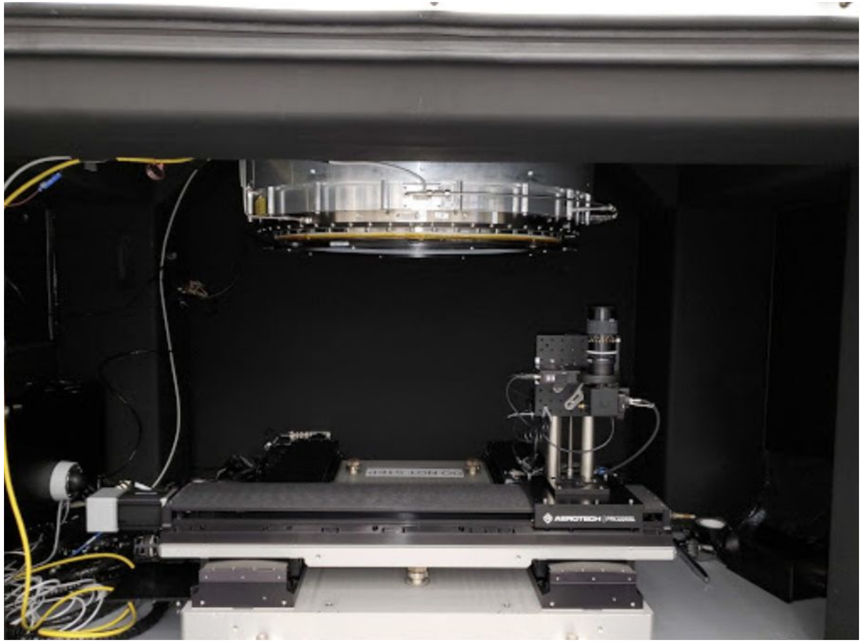

Spot projector
Image credit: Adam Snyder (UC Davis)
(Lab setup described in Newbry et al. 2018)

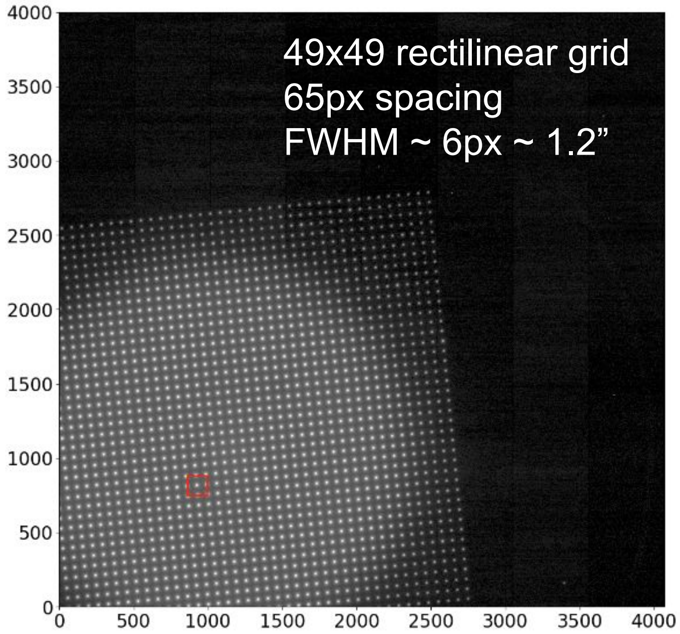

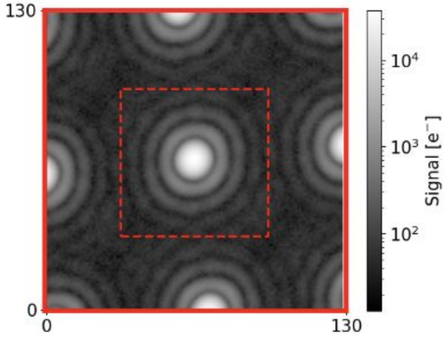

Broughton et al. (2023), Esteves et al. (2023)

Corrects 90% of the effect in stars

Corrects 77% of the anisotropy between x/y

I_{xx}

I_{yy}

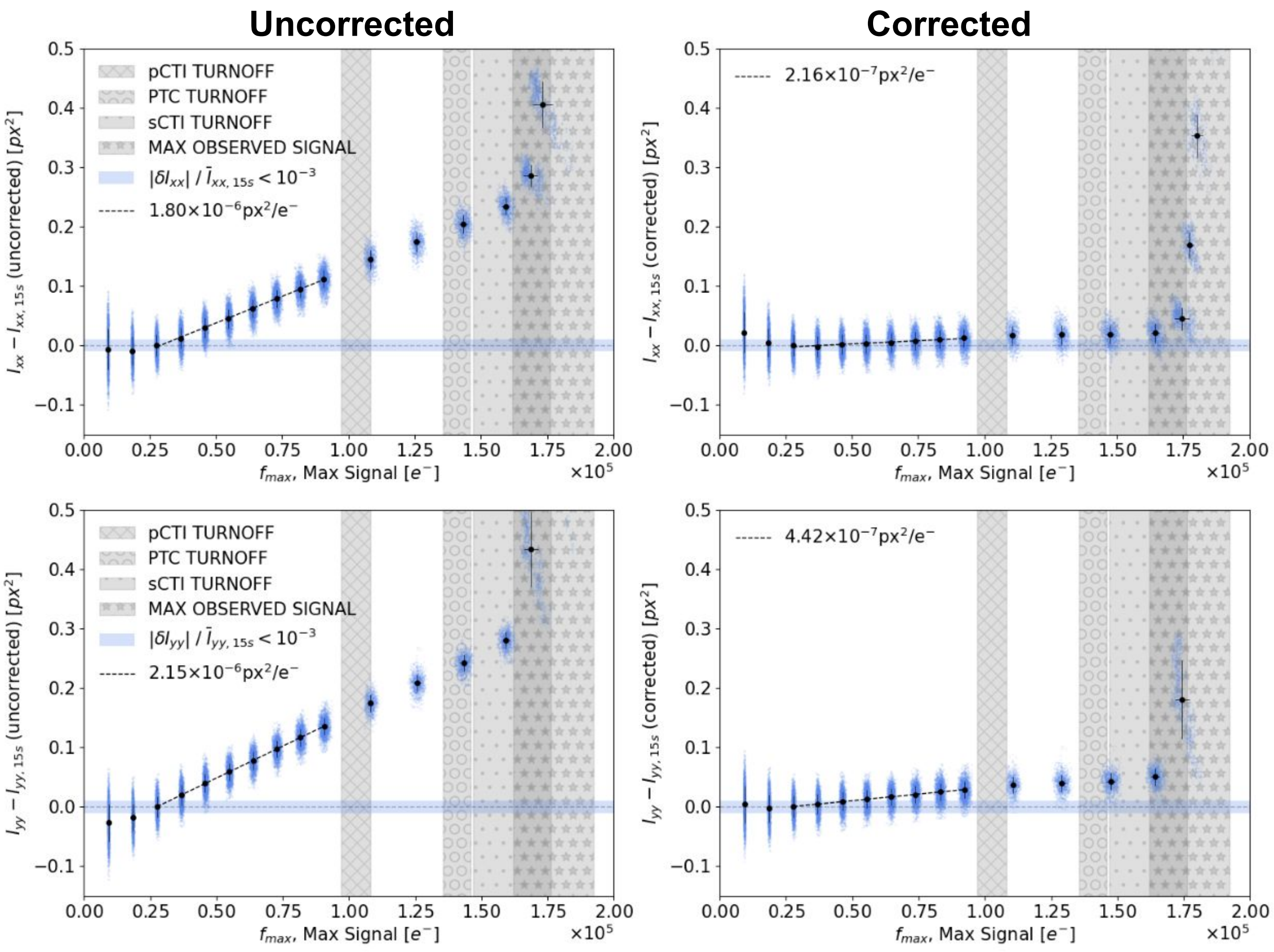

Broughton et al. (2023)

Why is the overall correction better in flat fields than in stars?

1. *Most of the correction is dominated by K_{00}, but realistically half of the BFE is contributed by correlations > 4px away*
2. *Unmodeled curl-component of displacement fields? (observed in HSC by Astier et al. 2023)*

$$c_{ij} = (a^N_{i+1,j} - a^N_{i,j}) - (a^E_{i,j+1} - a^E_{i,j})$$

3. *The application of the correction deviates from Gauss's Law on small scales, resulting in loss of charge conservation in stars*

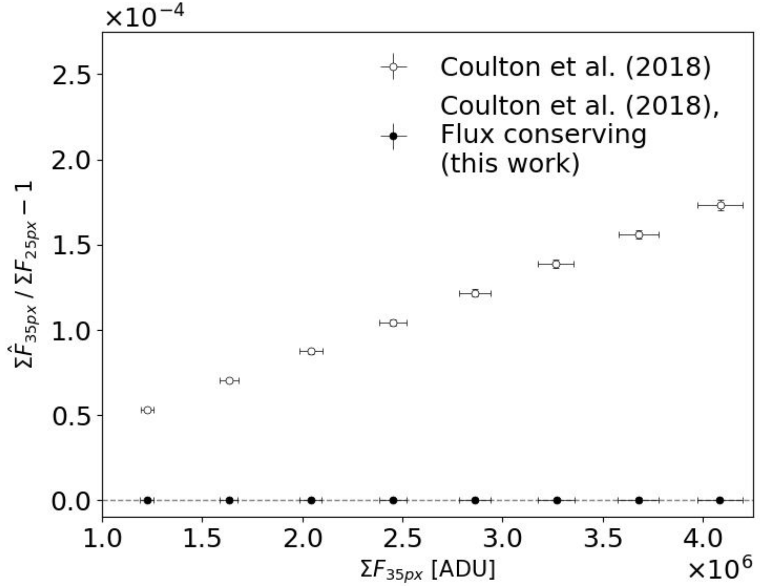

More flux is gained by the central pixels than is taken from the neighboring pixels

Flux is conserved, but only in the continuous limit

$$\langle \delta F \rangle = 0$$

Poor modeling of local charge transport=worse overall correction

Broughton et al. (2023)

Improvements can reconstruct true star size $T_* = \langle I_{xx} + I_{yy} \rangle$

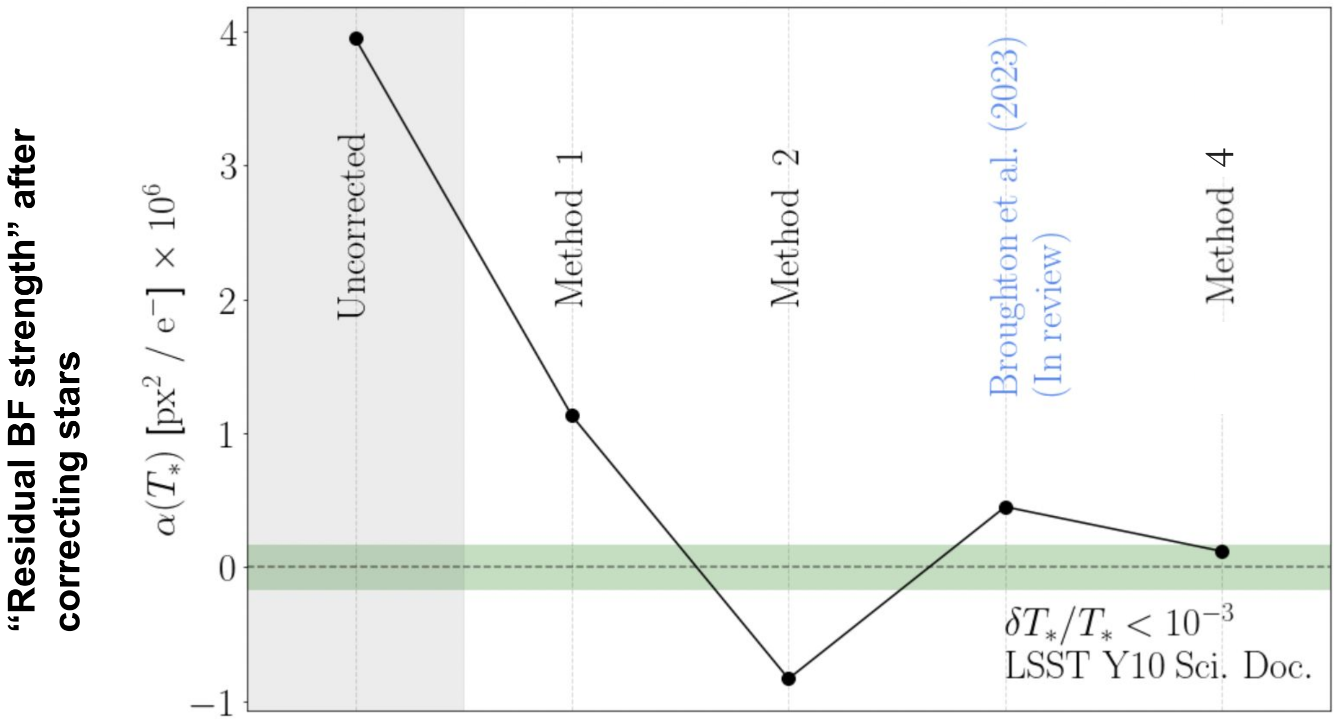

Method 1: Using kernel derived from high signal

Method 2: Using kernel derived from low signal

Method 3: Using kernel at the level that best reconstructs Poisson noise in flat fields.

Method 4: Method 3 + flux-conserving corrections (in prep.)

Last Notes

- The extensive and precise datasets provided by LSST will allow us to discriminate between imaging sensor systematics and new physics more clearly.
- Measurements of the amplitude of the BFE are sensitive to calibrations of other sensor artifacts that produce pixel correlations.
- Several corrections algorithms are being tested in LSSTCam: Antilogus et al. 2014, Gruen et al. 2015, Coulton et al. 2018, Astier et al. 2023.
  - Each makes varying assumptions about the symmetry and magnitude of different BFEs. All all require calibrated inputs of the amplitude of the BFE from flat field statistics.
  - Most modern survey experiments, regardless of correction algorithms, report approximately 10% residual effect on estimated PSFs